# Magnetic moment and lifetime of the first excited state of mirror nuclei $^{21}$Ne and $^{21}$Na

F. A. Beck, T. Byrski, G. J. Costa, and J. P. Vivien
*Centre de Recherches Nucléaires, 67037 Strasbourg Cedex, France*
(Received 21 March 1977)

The magnetic moment and lifetime of the first excited states of the mirror nuclei $^{21}$Ne and $^{21}$Na have been measured by the plunger-time differential-recoil-into-vacuum technique. The states were populated by the $^{4}$He($^{18}$O,$n$)$^{21}$Ne and $^{10}$B($^{16}$O,$\alpha n$)$^{21}$Na reactions at beam energies such that mainly three-electron recoil ions were produced. Values $|g| = 0.28 \pm 0.03$ and $|g| = 1.48 \pm 0.10$ have been deduced for the $^{21}$Ne and $^{21}$Na $g$ factors. The mean lifetimes of these states have been determined as $\tau = 10.1 \pm 0.3$ ps and $\tau = 9.9 \pm 0.4$ ps, respectively. The analysis of the measurements also provides information on atomic state populations in two, three, and four electron systems.

[NUCLEAR REACTIONS $^{4}$He($^{18}$O,$n$), $E = 19$ MeV; $^{10}$B($^{16}$O,$\alpha n$), $E = 42$ MeV; $^{2}$H($^{20}$Ne,$n$), $E = 14$ MeV; measured $\gamma(\theta,t)$ Doppler shift. $^{21}$Ne, 350 keV level and $^{21}$Na, 332 keV level, deduced $T_{1/2}$, $|g|$, ionic electron configurations.]

## I. INTRODUCTION

Hyperfine fields in one-electron systems are used extensively to measure magnetic moments of short lived states. However, few attempts have been made to utilize the hyperfine interaction occurring in stripped ions with more than two electrons.[1-3] In their first approach, Broude *et al.*[1] used a statistical model, taking into account all atomic configurations involving a $2s$ electron, to calculate the hyperfine field acting on the $^{16}$O nucleus. Later, in the case of $^{22}$Na, a model including the $p$ electron contributions and atomic configurations weighted according to their excitation probability was suggested.[2] A recent measurement of the ground state hyperfine splitting for Li-like fluorine[4] has shown the predominance of the $^{2}S_{1/2}$ atomic state. In addition a high recoil velocity $g$-factor measurement[5] also involving Li-like atoms gave information on atomic state populations.

The present paper reports $g$-factor measurements of the first $J = \frac{5}{2}^{+}$, $T = \frac{1}{2}$ states in the mirror nuclei $^{21}$Ne and $^{21}$Na. The recoil into vacuum measurements were performed at recoil energies such that mainly the three- and four-electron systems were populated. The results of the experiments show that a relatively small number of atomic configurations contribute to the interaction. They also demonstrate the feasibility of using the hyperfine interaction in three-electron systems to measure a large $g$ factor, the $1s$ one-electron frequency being too fast with respect to the plunger-time resolution. Concurrently the accurate lifetime determinations of the $J = \frac{5}{2}$ mirror states obtained in the present measurements considerably reduce the previous discrepancies observed with theoretical $B(M1)$ values. The magnetic properties $\mu$ and $B(M1)$ obtained for the two mirror nuclei are compared with available theoretical results.

## II. EXPERIMENTAL PROCEDURE

The time-differential perturbed angular correlation (TDPAC) method has been used in a recoil-distance arrangement to perform these measurements. The different electronic configurations that can be formed in the various ionic states following recoil from the target into a vacuum establish a superposition of hyperfine static fields acting on the nucleus during the nuclear lifetime.[2] The affected nuclei precess, giving rise to attenuation coefficients $G_k(t)$ in the $\gamma$-ray angular distribution[6]

$$W(\theta,t) = \sum_k A_k P_k(\cos\theta) G_k(t) , \tag{1}$$

$$G_k(t) = \sum_{FF'} \frac{(2F+1)(2F'+1)}{2J+1} \begin{Bmatrix} F & F' & k \\ I & I & J \end{Bmatrix}^2 e^{-i\omega_{FF'}t} , \tag{2}$$

where $\omega_{FF'} = (E_F - E_{F'})/\hbar$.

The detailed calculational procedure for $G_k(t)$ for the stopped fraction is given in Ref. 2.

The experimental setup was simplified by the fact that only the $G_2(t)$ variation had to be determined. Previous measurements had shown[7-9] that any $A_4$ term cannot be more than 0.005 for these $\frac{5}{2} \rightarrow \frac{3}{2}$ transitions.

Two Ge(Li) detectors were placed at 0° and 125° [$P_2(\cos\theta) = 0$]. Let $N_\theta$ be the measured stopped $\gamma$-ray intensity at the angle $\theta$. We can define

$$R(t) = \left(\frac{N_{0°}}{N_{125°}}(t)\right)_{\text{stopped}} \epsilon(D) , \tag{3}$$

where $\epsilon(D)$ is the relative detection efficiency, including geometric anisotropies of the two detectors. This quantity can be measured very precisely with a radioactive source positioned at the place of the stopper in the same mechanical configuration. Its variation with distance $D$ is very small. From expressions (1) and (3) we obtain

$$G_2(t) = \frac{R(t) - 1}{A_2 Q_2}. \tag{4}$$

The value of $A_2 Q_2$, where $Q_2$ is the geometrical attenuation coefficient of the detector positioned at 0°, was determined by performing an angular distribution measurement in which the recoiling nuclei were stopped in the target backing (10 $\mu$m Au) which was assumed to be free of hyperfine fields.

The first $^{21}$Ne excited state at 350 keV was populated in the reverse reaction $^4$He($^{18}$O, $n$)$^{21}$Ne at an $^{18}$O bombarding energy just below the threshold ($E_{th}$ = 19.2 MeV) of the long lived 2.79 MeV level ($J^\pi = \frac{1}{2}^-$). To check the fact that only the 350 keV level was excited, the yield of the stopped part of the 350 keV $\gamma$ ray was observed at a distance $D$ = 2000 $\mu$m. (This yield must be zero when there is no feeding from the 2.79 MeV state.) The targets used in the plunger measurements consisted of $^4$He implanted with a 50 keV energy generator into a 0.9 mg/cm$^2$ Ni layer for the first run and into a 3 mg/cm$^2$ Au layer for the second run. The angular distribution measured with $^4$He implanted into a 10 $\mu$m Au backing gave the result $A_2 Q_2 = -0.37 \pm 0.01$.

To excite the 332 keV mirror state in $^{21}$Na we chose the reaction $^{10}$B($^{16}$O, $\alpha n$)$^{21}$Na at $E_b$ = 42 MeV bombarding energy. Isotropic $^{10}$B targets, 100 $\mu$g/cm$^2$ thick, evaporated onto 1.5 mg/cm$^2$ Au backings were used for the plunger measurement. The anisotropy obtained for the angular distribution, measured with similar targets evaporated on 10 $\mu$m Au layers, was less than in the case of $^{21}$Ne: $A_2 Q_2 = -0.22 \pm 0.01$.

## III. RESULTS

### A. Lifetime measurements

The lifetime measurements were determined from the Doppler shifted intensity $I_s$ and the stopped peak $I_0$ observed in the detector positioned at 125°. Measurements made at this angle are insensitive to hyperfine field perturbations. The method of analysis has been described in detail elsewhere.[10]

Two runs were made for the first excited state of $^{21}$Ne. Data from the first, done with $^4$He implanted into Ni and illustrated in Figs. 1 and 2, gave $\tau$ = 9.9 ± 0.4 ps. The second one, done with $^4$He implanted into Au, yielded $\tau$ = 10.4 ± 0.5 ps. The mean value

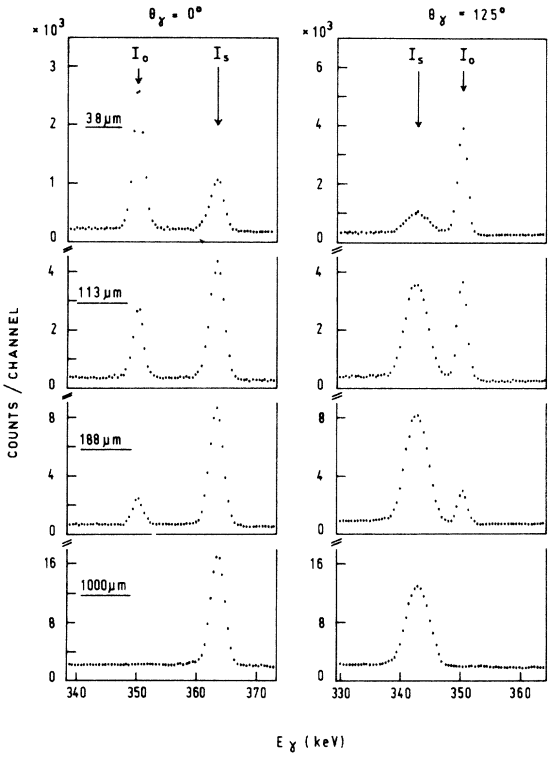


FIG. 1. Gamma-ray spectra for $^{21}$Ne recorded at $\theta_\gamma$ = 0 and 125° for various target stopper distances.

$\tau$ = 10.1 ± 0.3 ps is compared with previous measurements in Table I. Some disagreements appear with respect to these previous results but they may be explained by target problems due to deuterium absorption on the stopper (in Ref. 8), lack of statistics (in Ref. 9), and difficulties in the deduction of the contribution from the long lived 2.79 MeV state (in Ref. 11). The result reported in Ref. 12

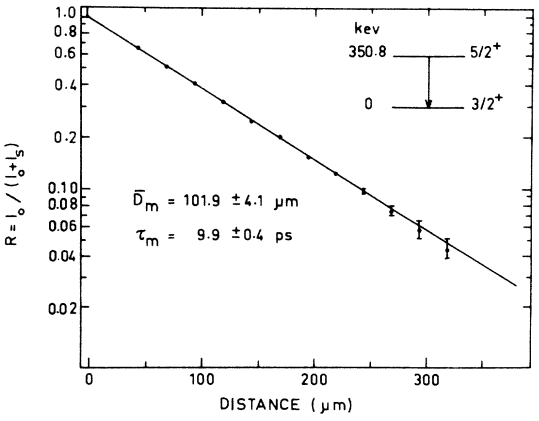


FIG. 2. Decay curve of the first excited state in $^{21}$Ne measured at $\theta_\gamma$ = 125°.

TABLE I. Measured lifetimes of the first excited states in $^{21}$Ne and $^{21}$Na.

| Reference | 350 keV ($^{21}$Ne) $\tau$ (ps) | 332 keV ($^{21}$Na) $\tau$ (ps) |
|---|---|---|
| 8 | 22 ± 3 | 14 ± 3 |
| 9 | 22.5 ± 1.0 | |
| 11 | 16 ± 4 | |
| 12 | 3.6 ± 1.0 | |
| 14 | 12.9 ± 1.6 | |
| This result | 10.1 ± 0.3 | 9.9 ± 0.4 |

has been measured by the DSAM method and it has been shown[13] that the slowing down material used gives lifetimes that are too short. A much better agreement is obtained with Ref. 14, although in the heavy ion reaction used, the $^{21}$Ne recoil ions have a large velocity distribution. This introduces an appreciable correction factor.

To avoid the velocity distribution problem in the measurement of the lifetime of the 332 keV $^{21}$Na state, we performed the measurement with the $^{2}$H($^{20}$Ne,$n$)$^{21}$Na reaction. The targets were 100 $\mu$g/cm$^2$ Ti$^2$H evaporated onto a 700 $\mu$g/cm$^2$ Ni foil. The $^{20}$Ne beam (14 MeV energy after traversing the Ni) was obtained at the Strasbourg 7 MV Van de Graaff accelerator. Two runs were made. The analysis, done separately or together as indicated in Fig. 3, led to the same mean result, $\tau = 9.9 \pm 0.4$ ps.

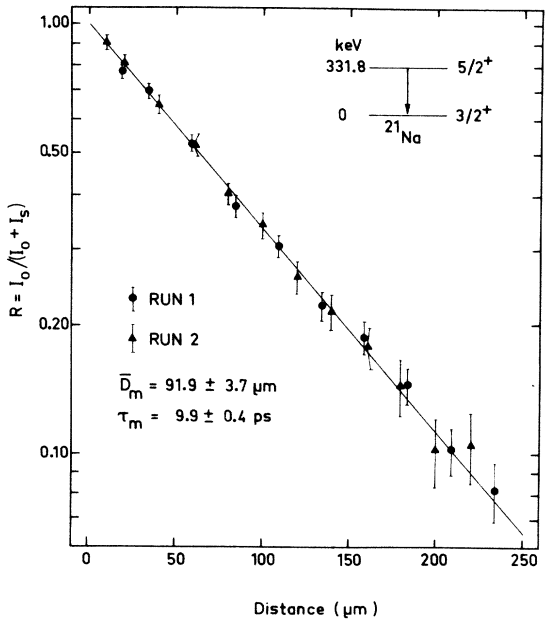


FIG. 3. Decay curve of the 332 keV level in $^{21}$Na obtained in the $^{2}$H($^{20}$Ne,$n$)$^{21}$Na reaction. The circles and triangles correspond to two different runs.

### B. Measurement of the $g$ factor

The measurements on Ne and Na were performed at recoil velocities $v/c = 3.49\%$ and 3.87%, respectively. This is close to the maximum yield of Li-like ions. In the Ne case, the corresponding charge state fractions $\phi$ deduced from measurements by Barrette, Knystautas, and Drouin[15] are $\phi(5^+) = 0.06$, $\phi(6^+) = 0.27$, $\phi(7^+) = 0.42$, $\phi(8^+) = 0.22$, and $\phi(9^+) = 0.02$.

For Na where no experimental charge state data are available, the fractions have been deduced from a Marion and Young[16] type calculation: $\phi(6^+) = 0.05$, $\phi(7^+) = 0.36$, $\phi(8^+) = 0.45$, and $\phi(9^+) = 0.14$.

Based on beam-foil measurements, it is expected that a large number of atomic levels in Li- and Be-like ions are populated. However, using the following arguments, the main contributions can be restricted to the $n = 2$ shell: In an ion-atom collision in the target, the favored states for an electron capture are those for which the ion velocity is comparable to the electron velocity. Then an ion of charge $\phi$ will have its main population in states

$$n \simeq (\phi + 1)[24.8 A_{\text{ion}}/E_{\text{ion}}(\text{keV})]^{1/2} . \tag{5}$$

Moreover many authors[17] have shown that the relative excited state production scales as $n^{-3}$. In addition, between $n = 2$ and $n = 3$ states there is a gap of about 100 eV in NeVII, NeVIII, and NaVIII and 150 eV in NaIX.

The possible $n = 1$ and $n = 2$ configurations and related terms for which the lifetimes are longer than the nuclear lifetime are listed in Table II. The indicated lifetime corresponds to the Ne case. These long lifetimes are due to forbidden decay modes like the $^3S_1 \rightsquigarrow {}^1S_0$ $M1$ transition and $^3P_2 \rightsquigarrow {}^1S_0$ $M2$ transition in the He isoelectronic sequence. In the Li sequence the $(1s, 2s, 2p)^3P_{2,1}$ terms, which can only deexcite via spin-interaction, spin-orbit, and spin-spin interactions, are metastable against autoionization.

The $g$-factor determination is deduced from the temporal behavior of the attenuation coefficient $G_2(t)$ in the angular distribution of the $\gamma$ rays. The calculated $G_2(t)$ results from the weighted superposition of the attenuation factors arising from each atomic term (cf. Table II) are

$$G_k(t) = \sum_{i,\alpha} P_{i\alpha} G_k^{i\alpha}(t) . \tag{6}$$

$P_{i\alpha}$ is the weight allotted to each term, and $G_k^{i\alpha}(t)$ is the corresponding attenuation coefficient.

As mentioned in Eq. (2), the $G_k(t)$ are related to the hyperfine energy splitting

TABLE II. Long lived $n=2$ atomic states in Ne. (For the decay schemes and lifetimes in Nevii and Neviii with $n>2$ see Ref. 30.)

| Ion | Configuration | Term | $\tau$ | Reference |
|---|---|---|---|---|
| Single electron | $1s^1$ | $^2S_{1/2}$ | $\infty$ | |
| Nex | $2s^1$ | $^2S_{1/2}$ | 120 ns | 18 |
| Two electron | $(1s)^2$ | $^1S_0$ | $\infty$ | |
| Neix | $(1s)^1(2s)^1$ | $^3S_1$ | 110 $\mu$s | 18 |
| | | | 91 $\mu$s | 19, 20 |
| | | $^1S_0$ | 115 ns | 18, 21 |
| | $(1s)^1(2p)^1$ | $^3P_0$ | 10 ns | 31 |
| | | $^3P_1$ | 140 ps | 22 |
| | | | 185 ps | 19, 23 |
| | | $^3P_2$ | 10 ns | 18, 19 |
| Three electron | $(1s)^2(2s)^1$ | $^2S_{1/2}$ | $\infty$ | |
| Neviii | $(1s)^2(2p)^1$ | $^2P_{1/2,3/2}$ | 1.47 ns | 24 |
| | | | 1.80 ns | 25 |
| | $(1s)(2s)(2p)$ | $^4P_{1/2}$ | ~2 ns | Extrapolated from 27 |
| | | $^4P_{3/2}$ | ~1 ns | 26 |
| | | $^4P_{5/2}$ | ~9 ns | Extrapolated from 27 |
| Four electron | $(1s)^2(2s)^2$ | $^1S_0$ | $\infty$ | |
| Nevii | $(1s)^2(2s)^1(2p)^1$ | $^1P_1$ | 241 ps | 28 |
| | | | 290 ps | 29 |
| | | $^3P_1$ | 62 $\mu$s | 19 |
| | $(1s)^2(2p)^2$ | $^1D_2$ | 2.02 ns | 29 |
| | | $^3P_{2,1,0}$ | 300 ps | 23 |

$$E_F=(-1)^{I+J+F}\begin{pmatrix} F & J & I \\ 1 & I & J \end{pmatrix} \times A_1 \Big/ \left[\begin{pmatrix} I & 1 & I \\ -I & 0 & I \end{pmatrix}\begin{pmatrix} J & 1 & J \\ -J & 0 & J \end{pmatrix}\right], \tag{7}$$

where $A_1$ is the magnetic hyperfine structure constant as defined by Schwartz[32]:

$$A_1=\frac{IJ}{|J(J+1)(J+2)|^{1/2}}\langle J||T_e^{\,1}||J\rangle . \tag{8}$$

For configurations involving identical electrons, the reduced matrix element in Eq. (8) can be found in the literature.[33-35] In the case of nonidentical electrons the expression for the $T_e^{\,1}$ matrix elements is given in a previous paper.[2]

Figure 4 represents the attenuation factor calculated for different atomic configurations for the Ne case. Table III gives the different values of $\langle r^{-3}\rangle$ and $|\psi(0)|^2$ introduced into the calculation of $G_k(t)$.

The $g$ factor was deduced from the experimental $G_2(t)$ curves by a nonlinear least squares fitting procedure. The zero distance of the plunger was determined separately and obtained from the lifetime data fit.

In a first approach, a calculation including all the possible long lived $[(1s)^2(2s)^n(2p)^m]$ $m,n=0,1,2$ states statistically weighted as in Ref. 1 was not able to reproduce the Ne data. The next step was to release the statistical weight condition and to fit with term weights varying independently. (The statistical weight condition was kept among members

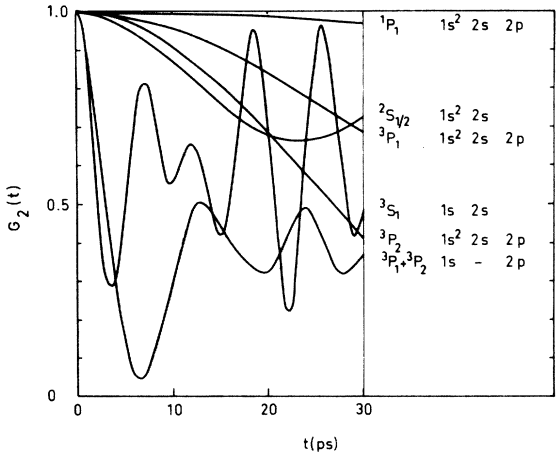


FIG. 4. Attenuation coefficient $G_2(t)$ computed for various configurations and terms of Ne ions. The calculation corresponds to a nuclear spin $I=\frac{5}{2}$ and a $g$ factor $g=0.3$.

TABLE III. Values in atomic units of $\langle r^{-3}\rangle$, $\langle r_I^{-3}\rangle$, $\langle r_{sc}^{-3}\rangle$, and $|\psi_0|^2$ used in the evaluation of the matrix element $\langle J||T_e^1||J\rangle$.

| Ion | Configuration | $\lvert\psi_0\rvert^2$ (a.u.) Ne | $\lvert\psi_0\rvert^2$ (a.u.) Na | $\langle r^{-3}\rangle$ (a.u.) Ne | $\langle r^{-3}\rangle$ (a.u.) Na |
|---|---|---|---|---|---|
| Two electron | $(1s)^1(2s)^1$ | 325.5 | 607.0 | | |
| Three electron | $(1s)^2(2s)^1$ | 29.8 | 41.0 | | |
| | $(1s)^2(2p)^1$ | | | 25.03 | 35.20 |
| Four electron | $(1s)^2(2s)^1(2p)^1$ | 27.6 | 38.4 | 23.00 | 32.65 |
| | $(1s)^2(2p)^2$ | | | 22.31 | 31.82 |

of the same multiplet.) This led to a considerable reduction in the number of participating terms. However, to reproduce the high frequency component one has to consider metastable states in He- and Li-like configurations with a hole in the $K$ shell.

In He-like ions the population among the strongly perturbing states $^3S_1$ and $^3P_{2,1}$ was first assumed to be statistical. Under this assumption one fixes an upper limit of 30% (at 3 standard deviations) of the total number of He-like ions which are in these excited states. A better agreement was obtained for the fit if only the $^3S_1$ state was taken into account. In such a case one finds $(25\pm10)\%$ of the two-electron systems in the $^3S_1$ state, the remaining $(74\pm14)\%$ being in zero field configurations $(1s)^2$ or $(1s)^1(2s)^1$ ($^1S_0$ term).

In Li-like ions one can set an upper limit of $(7^{+16}_{-7})\%$ of three-electron ions distributed among the $^2P_{1/2,3/2}$ states $[(1s)^2(2p)]$. The amount of three-electron ions in a $^4P$ state resulting from a $[(1s)(2s)(2p)]$ configuration was found to be less than 2%. This result is in agreement with a measurement by Sellin *et al.*[36] performed at the same reduced ionic velocity as in the neon case: $P_3=1$ (in charge state reduced units). These authors obtained for a 6 MeV $(5^+)$ O beam an occupation probability for the $[(1s)^1(2s)^1(2p)^1]$ $^4$P state of a few tenths of a percent per emergent Li-like ion.

In Be-like ions, the states that participate effectively in the perturbation are the $^3P_{2,1}$ terms of the $[(1s)^2(2s)(2p)]$ configuration. However, these metastable states induce a low frequency attenuation factor (see Fig. 4) and the fit for the $g$-factor determination is not very sensitive to the amount of the $^3P$ state relative to the $^1S_0$ ground state. The population ratio between the metastable and the ground states can be estimated as follows.

First of all, define the temperature of a plasma equivalent to a fast ion moving through a target by equating the plasma electron velocity to the projectile velocity. In final form a correction factor of 4 has been introduced by Nagel.[37] The equivalent temperature is then defined as

$$T_{eV}=90\frac{E}{A}\left(\frac{\text{MeV}}{\text{nucl.}}\right). \tag{9}$$

Knowing $T$, the Boltzmann equation can be used to calculate the population ratio between the metastable state and the ground state. The validity of the assumption of a Boltzmann distribution to calculafe the population of the metastable $^3P$ level was checked by Tondello and McWhirter[38] by measuring the intensity of the intercombination line $2s^2(^1S_0)-2s2p(^3P)$ in NeVII.

On the basis of experimental excitation rate coefficients[38] [the excitation rate coefficient of the $^1P(1s^22s2p)$ term is 6.5 larger than that of the $^3P(1s^22p^2)$ term] the $1s^22p^2$ configuration was not introduced in the calculation of $G_k(t)$.

In the B-like ions, in addition to the $^2P_{1/2}$ ground state, the metastable or long lived $^2P_{3/2}$ $\{[(1s)^2(2s)^2(2p)]$ configuration$\}$, $^4P$, $^2D$, $^2S$, and $^2P$ terms $\{[(1s)^2(2s)(2p)^2]$ configuration$\}$ were also introduced into the calculation. Due to the small contribution of B-like ions to the charge state distribution and their weak hyperfine interaction, the result of the fit is rather insensitive to the way the terms are weighted. In the final calculation a Boltzmann distribution was adopted for these terms.

Table IV summarizes the population of the different atomic states deduced from the Ne experiment along with the ionic recoil velocity (in charge reduced units) corresponding to each charge state of Ne and Na. The ionic velocity in reduced charge state units was introduced[39] to compare hyperfine interactions for stripped ions with velocities such that a given charge state fraction is the same. This parametrization is based on the fact that the charge state distributions plotted on a logarithmic scale have similar widths.[40] For each charge state $i$ one can therefore define the reduced velocity $P_i$ on a logarithmic velocity scale so that $P_i=1$ at the top of the charge distribution $i$. $P_i=1.5$ corresponds to the high velocity point at half maximum of the distribution and $P_i=0.5$ corresponds to the low velocity half maximum point.

TABLE IV. Population of electronic states in percent per charge state, measured in the $^{21}$Ne experiment. In the NeVIII case the population corresponds to a Boltzmann distribution with a temperature $T = 51$ eV. The numbers in the last column are the charge reduced velocity for the neon measurement and, in parentheses, the sodium experiment.

| Ion | Configuration | Term | Population (%) | Reduced ionic velocity | |
|---|---|---|---|---|---|
| NeIX | Zero field configurations $(1s^2, 1s^1 2s^1)$ | $^1S_0, {}^3P_0$ | $75 \pm 10$ | 0.43 | (0.3) |
| | $1s^1 2s^1$ | $^3S_1$ | $25 \pm 10$ | | |
| | $1s^1 2p^1$ | $^3P_{2,1}$ | | | |
| NeVIII | $1s^2 2s^1$ | $^2S_{1/2}$ | $93^{+7}_{-16}$ | | |
| | $1s^2 2p^1$ | $^2P_{1/2,3/2}$ | $7^{+16}_{-7}$ | 1.0 | (0.95) |
| | $1s^1 2s^1 2p^1$ | $^4P_{1/2,3/2,5/2}$ | $\leq 2$ | | |
| NeVII | Zero field configurations $(1s^2 2s^2, 1s^2 2s^1 2p^1)$ | $^1S_0, {}^3P_0$ | 27 | 1.38 | (1.32) |
| | $(1s^2 2s^1 2p^1$ | $^3P_{2,1}$ | 63 | | |
| | | $^1P_1$ | 10 | | |

Figure 5 represents the experimental data for $^{21}$Ne along with the fitted $G_2(t)$ corresponding to the population parameter of the atomic states discussed previously (see Table IV). The result of separate fits for each of the two runs gave the same $g$ factor as did the fit of the combined data. The sensitivity to the charge state fraction used in the calculation was checked. A 10% change in the charge state distribution did not significantly affect the $g$ factor. The final result for the $\frac{5}{2}^+$ $^{21}$Ne state is $|g| = 0.28 \pm 0.03$. This value takes into account a 5% possible error on the hyperfine field estimates.

In the Na case the $g$ factor was extracted in two different ways. First the reduced ionic velocities $P_2$, $P_3$, and $P_4$ being nearly the same as in the Ne case (see Table IV), the atomic population values of the Ne experiment were used in the $G_2(t)$ calculation (Fig. 6). The $g$ factor deduced from the fit is $|g| = 1.50 \pm 0.11$. Secondly, a frequency analysis of the data was performed. As shown in Ref. 4 the dominating frequency corresponds to the hyperfine splitting of the $^2S_{1/2}$ state in the Li-like atom. This procedure has the advantage of being independent of the exact charge state and atomic population values. The experimental $^2S_{1/2}$ hyperfine splitting reduced from the $G_2(t)$ data is

$$\omega_{FF'} = (9.21 \pm 0.42) \times 10^{11}$$

and corresponds to $|g| = 1.48 \pm 0.07$. In addition, a 5% error in the hyperfine field value has been included. The final value for the $\frac{5}{2}$ $^{21}$Na state is $|g| = 1.48 \pm 0.10$.

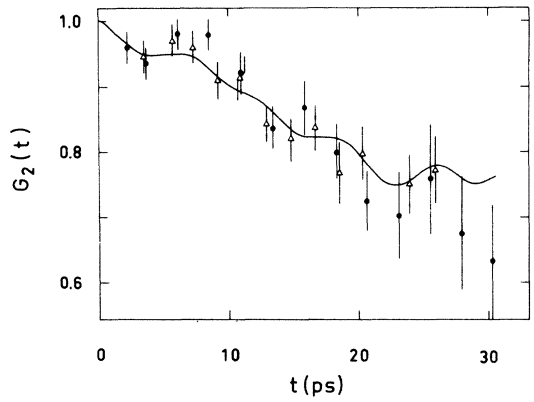


FIG. 5. Measured attenuation coefficient $G_2(t)$ for $^{21}$Ne. The circles and triangles correspond to two different runs. The curve represents the best fit to the two sets of experimental data.

## IV. DISCUSSION

The measured value and the theoretical estimates for the different magnetic properties of the $J^\pi = \frac{5}{2}^+$ state in the mirror nuclei $^{21}$Ne and $^{21}$Na are summarized in Table V. In both cases the measured lifetime differs significantly from published values (see Table I). The value obtained in this measurement considerably reduces the discrepancy with theoretical estimates especially for $B(M1)$ values. In the case of Ne with the $B(E2)$ value $(63 \pm 13$ $e^2\,\mathrm{fm}^4)$ as measured in Coulomb excitation by Schwalm and Povh,[49] one can extract the value of the mixing ratio $\delta(\frac{5}{2} \rightarrow \frac{3}{2}) = 0.064 \pm 0.007$ from the lifetime. This value is in agreement, within the error, with the value published by Pronko, Olsen, and Sample.[50] Using our lifetime and this mixing ratio, the value of the reduced transition probability deduced for the 350 keV transition in $^{21}$Ne is $B(M1) = (0.130 \pm 0.004)\mu_N{}^2$. The value $\delta = 0.05 \pm 0.02$ quoted in Ref. 7 has been utilized for $^{21}$Na to give $B(M1) = (0.156 \pm 0.006)\mu_N{}^2$.

Several theoretical $B(M1)$ estimates obtained

TABLE V. Magnetic properties of the $\frac{3}{2}^+$ and $\frac{5}{2}^+$ states in the mirror nuclei $^{21}$Ne and $^{21}$Na.

| Level ($J^\pi$) | Quantity | $^{21}$Ne Experimental values | $^{21}$Ne Calculated values | $^{21}$Na Experimental values | $^{21}$Na Calculated values |
|---|---|---|---|---|---|
| $\frac{5}{2}^+$ | $B(M1)$ $(\mu_N^2)$ | 0.130(4) [a] | 0.17 [b]<br>0.14 [d]<br>0.15 [c]<br>0.17 [e]<br>0.16 [f] | 0.156(6) [a] | 0.17 [c] |
| | $\mu$ $(\mu_N)$ | 0.70(7) [a] | −0.61 [g]<br>−0.52 [h] | 3.70(25) [a] | 3.38 [g]<br>3.40 [h] |
| $\frac{3}{2}^+$ | $\mu$ $(\mu_N)$ | −0.661762(5) [i] | 1.10 [d]<br>−0.55 [c]<br>−0.72 [f]<br>−0.77 [g]<br>−0.66 [h] | 2.38614(10) [j] | 2.83 [d]<br>2.144 [c]<br>2.44 [f]<br>2.50 [g]<br>2.41 [h] |

[a] Deduced from this measurement. The magnetic moments are in absolute values.
[b] Reference 42.
[c] Reference 44.
[d] Reference 43.
[e] Reference 45.
[f] Reference 46.
[g] Reference 47 (calculations with bare nucleon values).
[h] Reference 47 (calculations with fitted parameters).
[i] Reference 41.
[j] Reference 48.

with different models exist in the literature. The shell model calculation of Arima, Sakakura, and Sebe[43] using a truncated space and a $^{16}$O core is in good agreement for $B(M1)$ but is unable to account for the magnetic moment of the ground and first excited states in $^{21}$Ne and $^{21}$Na. The $B(M1)$ values nearest the experimental one are those obtained by Pronko, Lindgren, and Bromley[44] with a rotational model calculation including Coriolis bandmixing. However, the values they calculated for the ground state magnetic moment $\mu_{g.s.}$ of Ne and Na are, respectively, 20% and 10% too small. The projected Hartree-Fock calculations performed by Gunye[46] give a similar agreement for the $B(M1)$ but better values for $\mu_{g.s.}$

Recently Wildenthal and Chung[47] have performed a shell model calculation in a full *sd* space using modified Kuo matrix elements and a new method

TABLE VI. $g_0$ factor isoscalar part of the mirror nuclei $^{21}$Ne and $^{21}$Na.

| Level ($J^\pi$) | Experimental values | Calculated values |
|---|---|---|
| $\frac{3}{2}^+$ | 0.57479(2) [a] | 0.576 [b]<br>0.583 [c] |
| $\frac{5}{2}^+$ | 0.60(7) [d] | 0.576 [e]<br>0.554 [b]<br>0.576 [c] |

[a] Deduced from Refs. 41 and 48.
[b] Calculations from Ref. 47 with bare nucleon values.
[c] Calculations from Ref. 47 with fitted parameters.
[d] Deduced from the present measurements.
[e] Calculated with a pure $(d_{5/2})^5$ configuration.

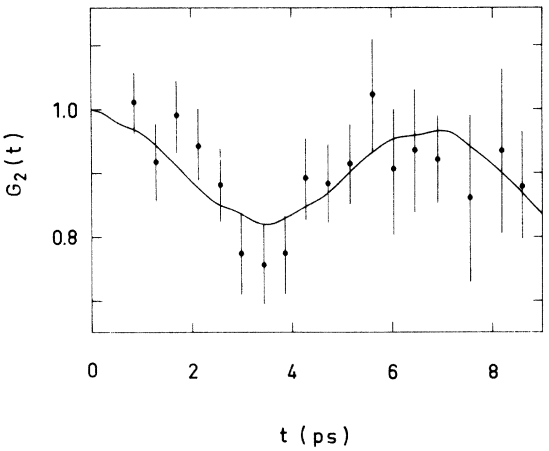


FIG. 6. The temporal behavior of $G_2(t)$ in the case of $^{21}$Na. The curve represents the best fit obtained using the atomic state populations deduced from the Ne measurements.

for fitting the energies in the $A = 18-24$ region. This calculation gives good results for the $^{21}$Ne and $^{21}$Na ground state magnetic moments. For the first excited state their values are a bit too small (1.3 standard deviations) for both nuclei. For a pair of mirror states, assuming charge independence of nuclear forces, one can extract the isoscalar part of the magnetic moment[51] from the measurement.

$$\mu_0 = g_0 J = \tfrac{1}{2} \left| \mu(A, T_z) + \mu(A, -T_z) \right| .$$

As was pointed out by van Hienen and Glaudemans,[52] for nuclei $A < 40$ the isoscalar part can be reproduced rather accurately with a simple $J^n$ configuration

$$g_0 = \frac{1}{2} \pm \frac{0.38}{2l+1} \quad \text{for } J = l \pm \tfrac{1}{2} .$$

Moreover, multishell mixed configurations do not produce considerably different results. Table VI shows the consistency of $g_0$ values extracted from the ground and first excited states of the $^{21}$Ne and $^{21}$Na pair, as well as values calculated for a $(d_{5/2})^5$ configuration and those derived from Wildenthal and Chung's calculation.[47]


[1]C. Broude, M. B. Goldberg, G. Goldring, M. Haas, M. J. Renan, B. Sharon, Z. Skedi, and D. F. H. Start, Nucl. Phys. A215, 617 (1973).
[2]F. Beck, Y. Dar, M. Forterre, and J. P. Vivien, Phys. Rev. C 13, 895 (1976).
[3]H. C. Jain, A. Little, S. M. Lazarus, T. K. Saylor, B. B. Triplett, and S. S. Hanna, Phys. Rev. C 14, 2013 (1976).
[4]W. L. Randolph, J. Asher, J. W. Koen, P. Rowe, and E. Matthias, Hyperfine Interaction 1, 145 (1975).
[5]R. E. Horstman, J. L. Eberhardt, H. A. Doubt, C. M.E. Otten, and G. Van Middelkoop, Nucl. Phys. A248, 291 (1975).
[6]K. Alder, Helv. Phys. Acta 25, 235 (1952).
[7]P. M. Endt and C. van der Leun, Nucl. Phys. A214, 1 (1973).
[8]A. Bamberger, K. P. Lieb, B. Povh, and D. Schwalm, Nucl. Phys. A111, 12 (1968).
[9]R. J. Nickles, Nucl. Phys. A134, 308 (1969).
[10]F. A. Beck, T. Byrski, P. Engelstein, and J. P. Vivien, Nucl. Phys. A228, 393 (1974).
[11]E. K. Warburton, J. W. Olness, G. A. P. Engelbertink, and K. W. Jones, Phys. Rev. C 3, 2344 (1971).
[12]D. C. Bailey, P. E. Carr, J. L. Durell, A. N. James, M. W. Greene, and J. F. Sharpey-Schafer, J. Phys. A 4, 908 (1971).
[13]C. Broude, F. A. Beck, and P. Engelstein, Nucl. Phys. A216, 603 (1973).
[14]H. H. Eggenhuisen, L. P. Ekström, G. A. P. Engelbertink, J. Mondria, M. A. Van Driel, and J. A. J. Hermans, Nucl. Phys. A246, 231 (1975).
[15]L. Barrette, E. J. Knystautas, and R. Drouin, Nucl. Instrum. Methods 110, 29 (1973).
[16]J. B. Marion and F. C. Young, *Nuclear Reaction Analysis* (North-Holland, Amsterdam, 1968).
[17]J. Davidson, Phys. Rev. A 12, 1350 (1975).
[18]R. Marrus, Nucl. Instrum. Methods 110, 333 (1973).
[19]C. Jordan, Nucl. Instrum. Methods 110, 373 (1973).
[20]G. W. F. Drake, Phys. Rev. A 3, 908 (1971).
[21]I. Martinson and A. Gaupp, Phys. Rep. 15C, 113 (1974).
[22]I. A. Sellin, M. Brown, W. W. Smith, and B. Donnally, Phys. Rev. A 2, 1189 (1970).
[23]W. L. Wiese, M. W. Smith, and B. M. Glennon, Nat. Stand. Ref. Data Ser., Nat. Bur. Stand. I, 4 (1966).
[24]J. P. Buchet, M. C. Buchet-Poulizac, G. Do Cao, and J. Desesquelles, Nucl. Instrum. Methods 110, 19 (1973).
[25]K. Berkner, W. S. Cooper, S. N. Kaplan, and R. V. Pyle, Phys. Lett. 16, 35 (1965).
[26]D. J. Pegg, H. Haselton, P. M. Griffin, R. Laubert, J. R. Mowat, R. Peterson, and I. A. Sellin, Phys. Rev. A 9, 1112 (1974).
[27]P. Richard, in *Atomic Inner Shell Processes*, edited by E. B. Crasemann (Academic, New York, 1975).
[28]D. J. G. Irwin, A. E. Livingston and J. A. Kernahan, Nucl. Instrum. Methods 110, 105 (1973).
[29]G. Beauchemin, J. A. Kernahan, E. Knystautas, D. J. G. Irwin, and R. Drouin, Phys. Lett. 40A, 194 (1972).
[30]L. Barrette and R. Drouin, Phys. Scr. 10, 213 (1974).
[31]H. Gould and R. Marrus, in *Proceedings of the Fourth International Conference on Beam Foil Spectroscopy, Gatlinburg, 1975*, edited by I. A. Sellin and D. J. Pegg (Plenum, New York, 1976).
[32]C. Schwartz, Phys. Rev. 97, 380 (1955).
[33]G. K. Woodgate, Proc. R. Soc. 293, 117 (1966).
[34]J. Bauche and B. R. Judd, Proc. Phys. Soc. 83, 145 (1964).
[35]L. Armstrong, *Theory of the Hyperfine Structure of Free Atoms* (Wiley-Interscience, New York, 1971).
[36]I. A. Sellin, D. J. Pegg, M. Brown, W. W. Smith, and B. Donnally, Phys. Rev. Lett. 27, 1108 (1971).
[37]D. J. Nagel, in *Proceedings of the Fourth International Conference on Beam Foil Spectroscopy, Gatlinburg, 1975* (see Ref. 31).
[38]G. Tondello and R. W. P. McWhirter, J. Phys. B 4, 715 (1971).
[39]H. A. Doubt, Haifa International Workshop on Topics in Atomic Physics Related to Nuclear Experimentation, Haifa, August, 1976 (unpublished).
[40]G. Goldring, Weizman Institute of Science Report No. Wis 75/57 PH, 1975 (unpublished).
[41]J. T. Latourette, W. E. Quinn, and N. F. Ramsey, Phys. Rev. 107, 1202 (1957).
[42]E. G. Halbert, J. B. McGrory, B. H. Wildenthal, and S. P. Pandya, in *Advances in Nuclear Physics*, edited by M. Baranger and E. Vogt (Plenum, New York, 1971), Vol. 4, p. 315.
[43]A. Arima, M. Sakakura, and T. Sebe, Nucl. Phys. A170, 273 (1971).
[44]J. G. Pronko, R. A. Lindgren, and D. A. Bromley, Nucl. Phys. A140, 465 (1970).
[45]J. Hiura, F. Nemoto, and H. Bando, Prog. Theor. Phys. Suppl. 52, 173 (1972).
[46]M. R. Gunye, Phys. Rev. C 7, 216 (1973).

[47]B. H. Wildenthal and W. Chung, Michigan State University, private communication.
[48]O. Ames, E. A. Phillips, and S. S. Glikstein, Phys. Rev. 137, 1157 (1965).
[49]D. Schwalm and B. Povh, in *Proceedings of the International Conference on Properties of Nuclear States, Montréal, 1969*, edited by M. Harvey *et al.* (Presses de l'Université de Montréal, Montréal, Canada, 1969).
[50]J. G. Pronko, W. C. Olsen, and J. T. Sample, Nucl. Phys. 83, 321 (1966).
[51]I. Talmi, in *Hyperfine Interactions in Excited Nuclei*, edited by R. Kalish and G. Goldring (Gordon and Breach, New York, 1971), p. 1133.
[52]J. F. A. van Hienen and P. W. M. Glaudemans, Phys. Lett. 42B, 301 (1972).